Continuous vs Discontinuous Capillary Desaturation and Implications for IOR/EOR

Rui Xu, Bernd Crouse, David M. Freed, Andrew Fager, EXA CORP
Gary R. Jerauld, Nathan Lane, Qiang Sheng, BP

This paper was prepared for presentation at the International Symposium of the Society of Core Analysts held in Trondheim, Norway, 27-30 August 2018

ABSTRACT

Enhanced oil recovery (EOR) methods are designed to increase oil recovery after secondary, and sometimes primary, recovery. EOR methods often aim to increase the Capillary number (Nc), which represents the balance between viscous and capillary forces in the multi-phase-fluid-rock system, either by decreasing the interfacial tension (IFT) between oil and water phases (surfactant injection) or by increasing the viscosity of the water phase (polymer injection). Capillary desaturation curves (CDC) show the influence of capillary number on remaining oil and hence can be used to study displacement efficiency and physical parameter sensitivities relevant to recovery. The ability to predict the impact of a particular EOR approach on microscopic sweep efficiency for specific rock types can help reduce uncertainty during the planning and execution of a project.

In this study CDC's are generated using digital rock pore-scale flow simulations on a Berea sandstone. Two different displacement processes were conducted: continuous and discontinuous displacement. The continuous CDC method involves a series of waterflooding simulations. Separate simulations are conducted, each with the same initial fluid distribution close to irreducible water saturation but at different capillary numbers. Remaining oil saturation to waterflood is then measured for each simulation. In the discontinuous CDC method an initially small capillary number is simulated for set number of injected pore volume. Then the capillary number is increased in a step-wise fashion (bumped) and a new oil saturation is measured for each 'bump' in capillary number. Continuous and discontinuous CDC's are herein compared for two wetting configurations, water-wet and oil-wet, using the same digital rock sample.

For the water-wet rock, the critical capillary number (the largest capillary number below which the viscous forces no longer affect oil production) was smaller for the continuous CDC than for the discontinuous CDC. This observation is consistent with previous findings from laboratory coreflood tests indicating that the continuous displacement process is typically the more efficient method. For oil-wet rocks it was observed that the CDC is a function of injected pore volume because oil continues to be produced as water is injected. At low Nc it was observed that oil-wet gives better recovery than water-wet, while this trend is reversed at higher Nc. The results of this study demonstrate that the

digital rock approach is able to capture sensitive trends such as wettability, history, and capillary number effects that occur during water floods.

INTRODUCTION

During the life of an oil field several production stages may be encountered. In the primary recovery stage, oil flows naturally to the wells due to the high reservoir pressure underground. Over time the reservoir pressure drops, and secondary recovery may be performed, where water or gas are injected to increase pressure and displace more oil. A tertiary recovery stage may be able to recover additional oil using Enhanced Oil Recovery (EOR) methods [1][2][3]. Results from Special Core Analysis Laboratories, such as relative permeability and capillary pressure curves are key inputs to the reservoir models used to estimate the recovery efficiency and make economic decisions about a reservoir. The ability to assess the impact of variations in viscosity, wettability, IFT and flow rate on the reservoir model inputs is essential to understanding and bounding the uncertainty of the results from those models. The capillary desaturation curve (CDC) can be used to characterize one such sensitivity [4].

A CDC gives the amount of trapped oil as a function of capillary number for a given rock sample [4][5]. CDC is strongly affected by wettability with weakly water-wet or mixed-wet conditions often leading to maximum oil recovery [6-11]. Remaining oil may also be affected by whether the displacement process is continuous or discontinuous. It has been reported that displacing discontinuous (trapped) oil blobs can be 10 times more difficult than displacing continuous oil [5][12]. These effects will manifest themselves in a CDC.

Changes in flow-rate, viscosity and IFT can all be represented by changes in the dimensionless capillary number (Nc), which represents the ratio of viscous to capillary forces. There are a few common expressions for capillary number [2,13,14]; the expression used in this study is

$$\mathrm{Nc} = \frac{k_w \frac{\Delta P}{L}}{\sigma} \tag{1}$$

In Equation (1), k_w is the absolute permeability of the water phase, $\Delta P/L$ is the pressure gradient, and σ is the oil/water interfacial tension (IFT). Usually a CDC will reveal a critical capillary number (Ncc), such that for Nc below Ncc the remaining oil saturation is constant. For Nc above Ncc the remaining oil saturation tends to monotonically decrease with increasing Nc, signifying increasing oil recovery.

In this study CDC's are generated using digital rock pore-scale flow simulations on a Berea sandstone. The commercially available DigitalROCK® software is used to simulate the water-oil displacement process at the pore-scale. The pore space geometry is obtained from a 3D micro-CT image [15,16] and used as input to the multi-phase flow simulation solver, which is based on the Lattice-Boltzmann method and validated for a broad range of fundamental test cases as well as reservoir sandstones [16-24].

Two different displacement processes were investigated: continuous and discontinuous. The continuous CDC method involves a series of unsteady-state relative permeability simulations. Separate simulations are conducted, each with the same initial fluid distribution (near irreducible water saturation) but at different capillary numbers. Remaining oil saturation is then measured for each simulation. In the discontinuous CDC method an initially small capillary number is simulated until remaining oil saturation is achieved. Then the capillary number is increased in a step-wise fashion (bumped) and a new saturation is measured for each 'bump' in capillary number. Continuous and discontinuous CDC's are herein compared for two wetting configurations, water-wet and oil-wet, using the same digital rock sample.

MEASUREMENTS AND PROCEDURE

Rock Sample Scan

A small plug of Berea Sandstone was imaged (Figure 1) with a micro-CT scanner using a resolution of 2.02um/voxel-edge. The resulting 3D image of the grains and pore space was denoised and segmented using typical image processing techniques including contrast enhancement, low-pass filtering and thresholding [25]. A resolved porosity ϕ=15.7% was determined, and an absolute permeability of 235mD was obtained from a single-phase flow simulation. A cubic domain of size 500x500x500 voxels was used as the digital sample in this study.

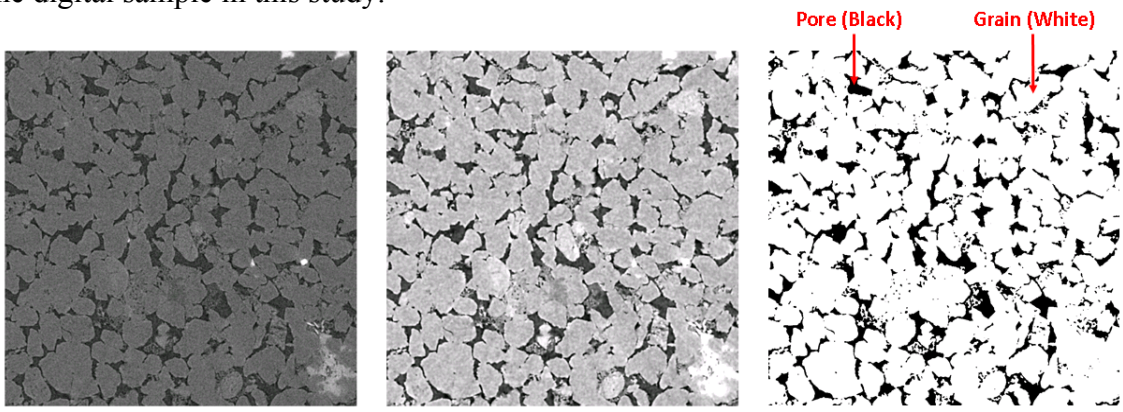

Figure 1. Berea Sandstone micro-CT: original, denoised, and segmented image slices.

Multi-Phase Flow Simulations - Initial Fluid Distribution and Wettability

An initial water saturation (Swi) of 10% was chosen for all simulations. A drainage process was used to determine the locations of initial water and oil. Then, pore surfaces in contact with initial water were assigned a contact angle of 10°, reflecting the strongly water-wet nature of surfaces associated with connate water. Pore surfaces in contact with initial oil assigned contact angle 30° for the water-wet condition and 150° for the oil-wet condition (Figure 2). This strategy emulates the wettability alteration process for fluid-contacted reservoir rock. The simulated Amott indices were Iw=0.9, Io=0.06 for the water-wet condition and Iw=0, Io=0.34 for the oil-wet condition. These Amott indices are typical for water-wet and oil-wet conditions, indicating that the choice of contact angles is reasonable [26].

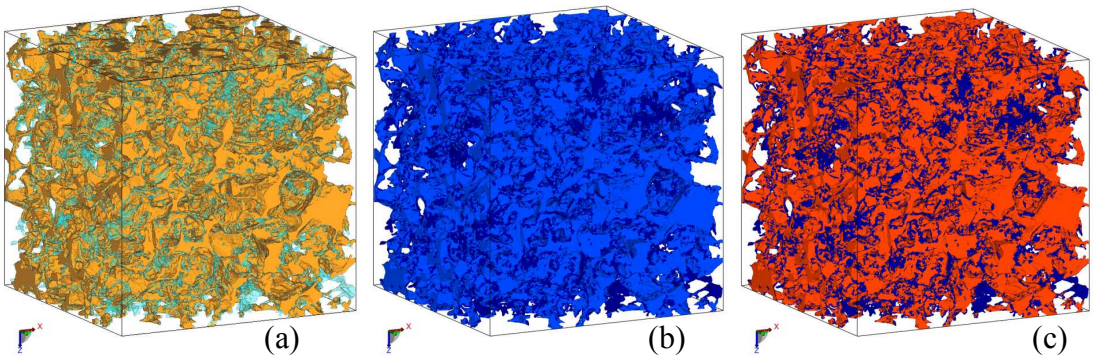

Figure 2: (a) Initial distribution of oil [yellow] and water [light-blue], (b) visualization contact angle distribution for of water-wet and (c) oil-wet wetting cases [dark-blue: 10°, light blue: 30°, red: 150°]

Multi-Phase Flow Simulations - Waterflooding

The same digital rock sample with the same initial fluid distribution was used for all waterflood simulations throughout this study. For the continuous oil displacement method:

- Each independent flood was performed at a different pressure gradient resulting in a different capillary number.
- For the water-wet condition, simulations were run to Sor as determined by verifying that all remaining oil is trapped and immobile.
- For the oil-wet condition, the remaining oil saturation is a function of the number of pore volumes of water injected, since remaining oil usually does not become fully immobilized due to the presence of connected oil films. Therefore, a specified volume of water was injected for each flood.

For the discontinuous oil displacement method:

- A first flood was performed at a low-pressure gradient.
- This was followed by multiple stepwise pressure increases.
- Each increase led to a higher capillary number than previously achieved.
- For water-wet condition, for each pressure increment, water was injected until no further oil was produced and the saturation profile converged in time.
- In the oil-wet case, pressure was increased after 1 PV water injection, which was found to be sufficient to characterize the capillary number dependence.

RESULTS AND DISCUSSION

Continuous Oil Displacement in Water-Wet Case

Oil is displaced continuously in each individual flooding test. Remaining oil saturations were observed to be constant after injection of 0.7 to 2.5 PV's of water. For the lowest capillary number (2.2E-5) a converged water saturation profile and remaining oil saturation was reached after injecting 0.7 PV of water (Figure 3a). For high capillary number more PV's are needed to displace all movable oil. This is due to the higher viscous forces present at high capillary number. In Figure 3b, saturation profiles at remaining oil saturation along the flow direction are plotted for each capillary number.

3D remaining oil distributions after continuous displacement for each capillary number are shown in Figure 4. These visualizations display oil as gold, water as blue, and solid grains are not shown.

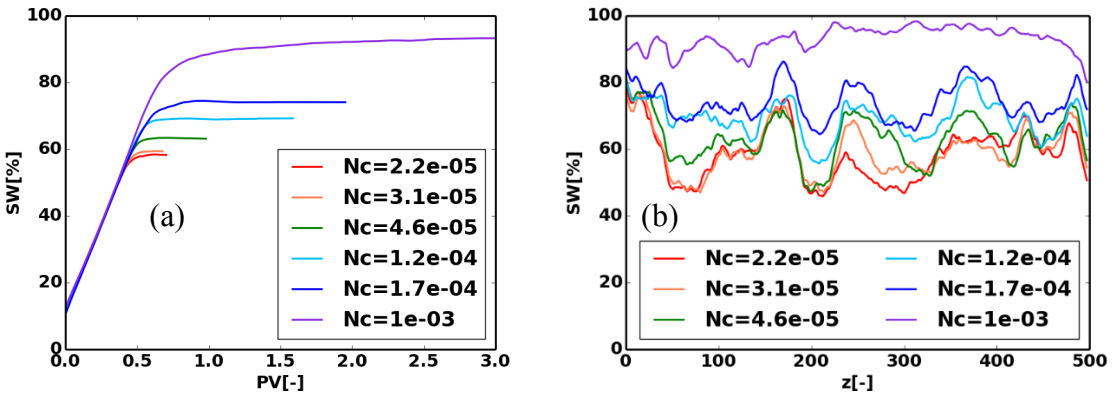

Figure 3: (a) Water saturation as a function of injected water (b) water saturation profile in flow direction

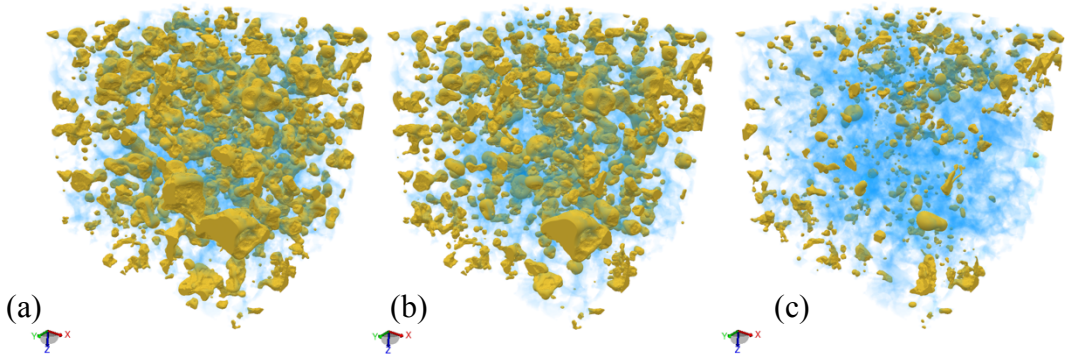

Figure 4: Remaining oil distribution after continuous displacement at capillary number (a) Nc = 2.2e-5, (b) Nc = 1.2e-4, (c) Nc = 1e-3.

Discontinuous Oil Displacement in Water-Wet Case

Water is injected at low pressure with Nc = 2.2e-5 and then pressure is increased in steps (Figure 5). Before each pressure increase, immobilization of remaining oil saturation was confirmed; note that in pore-scale simulations, such convergence can be detected accurately and rapidly since the fluid distributions throughout the pore space are known precisely at each instant. For some capillary numbers this allowed reduced water volume injection compared to typical laboratory tests. Figure 6 shows 3D remaining oil distributions after discontinuous displacement for each capillary number. From these visualizations one can see locations where oil blobs were mobilized and removed after a pressure gradient increase.

Figure 7a shows the CDC curves for both continuous and discontinuous displacements under water-wet conditions. The discontinuous CDC shows a higher critical capillary

number (Ncc) than the continuous CDC. Both CDC curves eventually merge at high capillary number (Nc>6E-4). These observations are consistent with previous studies conducted in the laboratory [5][12]. Figure 7b shows the present results plotted together with analogous lab test CDC results reported by Chatzis & Morrow on a Berea sample [5]; the trends are clearly very similar.

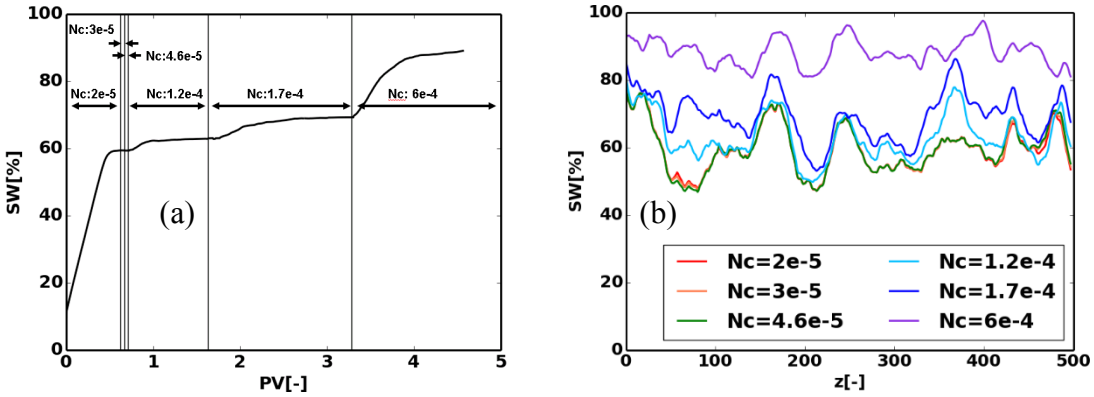

Figure 5: (a) Water saturation vs. pore volume for discontinuous displacement, water-wet. (b) water saturation profile in flow direction for discontinuous displacement, water-wet

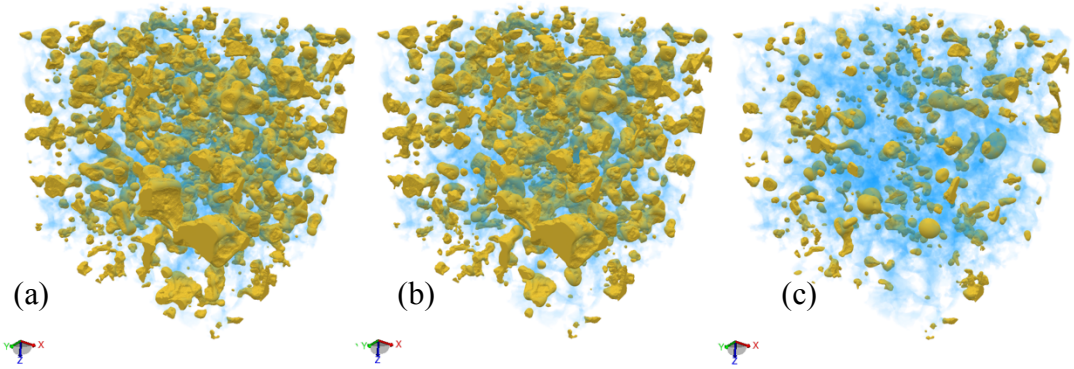

Figure 6: Remaining oil distribution at capillary (a) Nc = 2.2e-5(lowest), (b) Nc = 1.2e-4, (c) Nc = 6e-4 (highest) by discontinuous displacement

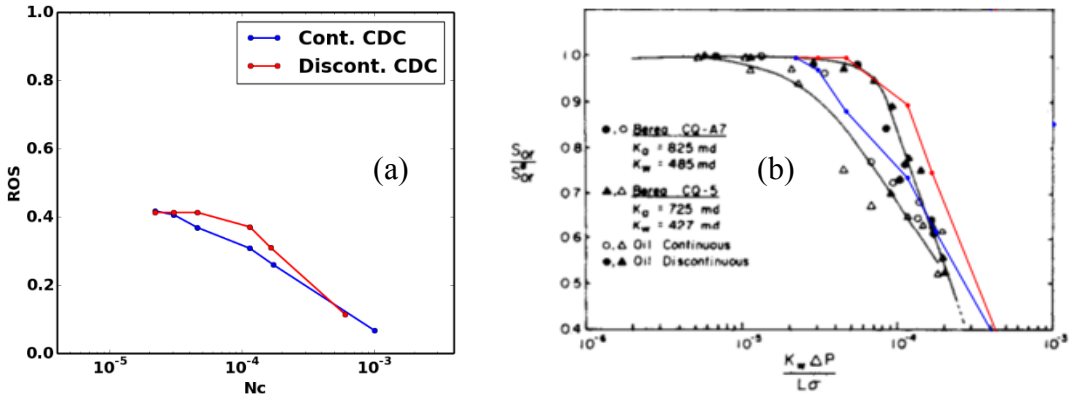

Figure 7: (a) CDC for continuous (blue) and discontinuous (red) oil displacement, (b) Present CDC results compared to lab test results of Chatzis & Morrow [5]

Continuous Oil Displacement in Oil-Wet Case

Figure 8a shows water saturation as a function of injected pore volume for continuous displacement. As noted previously, for displacement in the oil-wet rock, a final Sor is typically not achieved due to ongoing oil production attributed to film flow. It is observed here that, as expected, the remaining oil saturation decreases (oil recovery increases) as more water is injected. Figure 8b shows saturation profiles along the flow direction at 5PV's injection volume. Figure 9 shows the corresponding remaining oil distribution for similar Nc values shown in Figure 6 (for water-wet). Figure 10 shows that the continuous CDC behavior is noticeably different for oil-wet compared to water-wet. The oil-wet critical capillary number (Ncc) is around 7.4e-5 and higher than that for water-wet. The oil-wet case results in more oil recovery than water-wet at low capillary number, but as capillary number increases, the remaining oil behavior changes and the water-wet case gives better recovery. These observations are consistent with previously published results [7,9,10,27]. Also shown in Figure 10 is the oil-wet CDC for different volumes of injected water; as the injection volume increases, the remaining oil decreases, as observed in experimental studies [9].

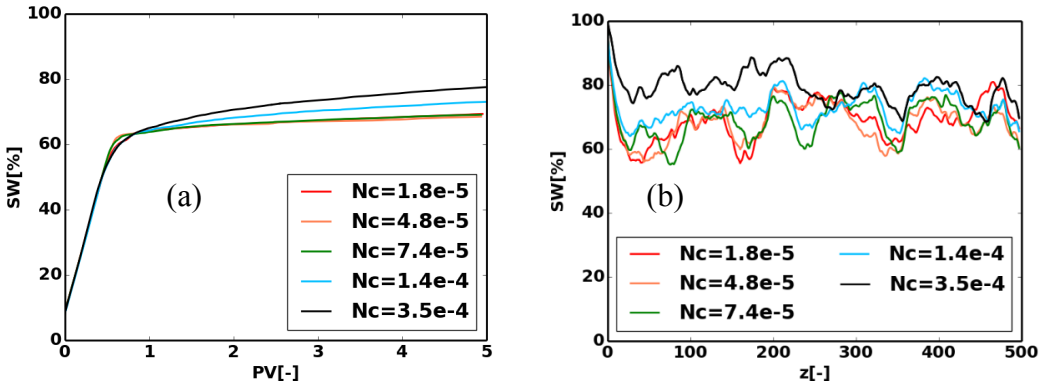

Figure 8: (a) Water saturation as a function of injected water (b) Water saturation profile in flow direction

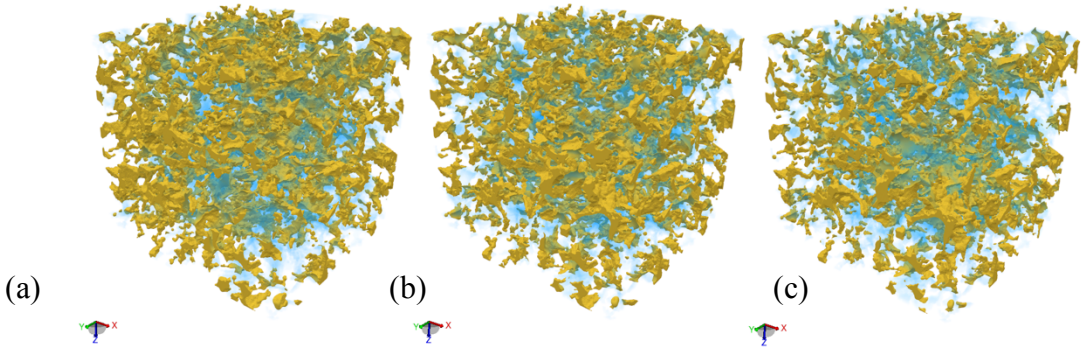

Figure 9: Remaining oil after 5PV of water injection for capillary number (a) Nc = 1.8e-5(lowest), (b) Nc = 1.4e-4, (c) Nc = 3.5e-4(highest) by continuous displacement

Discontinuous Oil Displacement in Oil-Wet Case

As with the continuous oil-wet case, for discontinuous displacement the stepwise pressure increments were applied at predetermined PV's. Here 2.5 PVs were injected at the lowest capillary number before increasing pressure. All subsequent pressure increases were applied after an additional 1 PV of injection (Figure 11). The results show that changing the pressure increased mobility of oil, however, it is difficult to distinguish recovery due to increased pressure versus recovery due to increased water injection for the discontinuous oil-wet CDC.

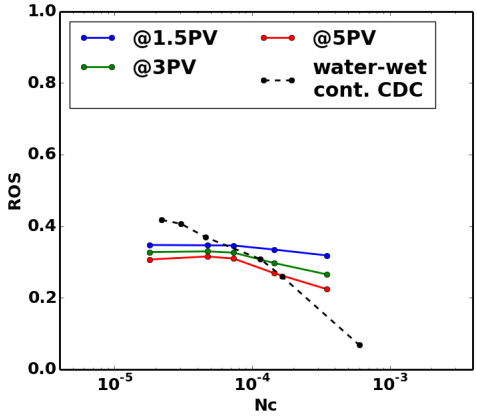

Figure 10: continuous CDC for oil-wet rock at 1.5pv, 3pv and 5pv vs water-wet.

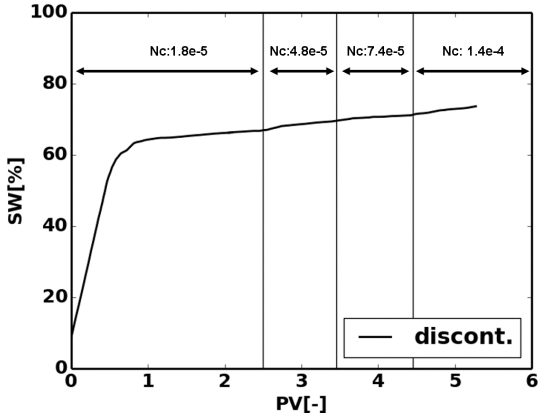

Figure 11: Water saturation vs. pore volume for discontinuous displacement, oil-wet. Pressure was increased at 2.5, 3.5, 4.5 PVs.

CONCLUSION

Using a digital rock physics simulation approach, capillary desaturation curve (CDC) behavior was shown for discontinuous and continuous displacement methods for both water-wet and oil-wet conditions. The resulting CDC's confirm that the critical capillary number is larger for the discontinuous CDC method, indicating a less efficient displacement process. It was further shown, that the critical capillary number tends to be larger for oil-wet rocks than for water-wet rocks, and that the remaining oil saturation of oil-wet rocks tends to be smaller at low capillary numbers. These results are consistent with previously reported results from experimental lab testing. Important trends for microscopic sweep efficiency, such as continuous versus discontinuous displacement, water-wet versus oil-wet rocks, and low versus high capillary numbers, are correctly captured by the simulation approach used herein based on the commercial software DigitalROCK. Such pore-scale sweep efficiency trends are of critical importance in assessing the potential for EOR methods to provide incremental oil recovery. Moreover, sensitivity studies allowing an understanding of the impact of key parameter variations can be performed rapidly with digital methods.

ACKNOWLEDGEMENTS

Many thanks to BP's Center for High-Performance Computing (CHPC) for providing computational resources for this study.

REFERENCES

[1] Meyer, J.P., "Summary of Carbon Dioxide Enhanced Oil Recovery (CO2EOR) Injection Well Technology", *American Petroleum Institute*, (2007), p. 54.
[2] Al-Mjeni, R & Arora, S & Cherukupalli, P & Van Wunnik, J & Edwards, J & Felber, B.J. & Gurpinar, Omer & Hirasaki, G & Miller, Clarence & Jackson, C & Kristensen, Morten & Lim, F & Ramamoorthy, Raghu, "Has the time come for EOR?" *Oilfield Review*, (2011) **22**, p. 16-35
[3] Lake, L.W. 1989. *Enhanced Oil Recovery*, Englewood Cliffs, New Jersey: Prentice Hall, 314-353.
[4] Yeganeh, M., Hegner, J., Lewandowski, E., Mohan, A., Lake, L.W., Cherney, D., … Jaishankar, A., "Capillary Desaturation Curve Fundamentals", *Society of Petroleum Engineers*, (2016).
[5] Chatzis, I., & Morrow, N.R., "Correlation of Capillary Number Relationships for Sandstone", *Society of Petroleum Engineers*, (1984, October 1).
[6] Maldal, T., Jakobsen, R., Alvestad, J., Arland, K.S., "Relationship Between Remaining Oil Saturation After Waterflooding and Rock Flow Properties at Laboratory and Reservoir Scale", *Petroleum Geoscience*, (1999) **5**, p. 31-35.
[7] Humphry, K.J., Suijkerbuijk, B.M.J.M., van der Linde, H.A., Pieterse, S.G.J., & Masalmeh, S.K., "Impact of Wettability on Residual Oil Saturation and Capillary Desaturation Curves", *Society of Petrophysicists and Well-Log Analysts*, (2014).
[8] Johannesen, E.B., & Graue, A., "Mobilization of Remaining Oil - Emphasis on Capillary Number and Wettability", *Society of Petroleum Engineers*, (2007, January 1).
[9] Abeysinghe, K.P., Fjelde, I., & Lohne, A., "Dependency of Remaining Oil Saturation on Wettability and Capillary Number", *Society of Petroleum Engineers*, (2012).
[10] Tanino, Y. and Blunt, M.J. , "Laboratory investigation of capillary trapping under mixed-wet conditions", *Water Resources Research*, (2013) **49**, number 7, p. 4311--4319
[11] Anderson, W.G., "Wettability Literature Survey-Part 6: The Effects of Wettability on Waterflooding", *Journal of Petroleum Technology*, (1987) **39**, p. 1605-1622.
[12] Stegemeier, G.L., "Mechanisms Of Entrapment And Mobilization Of Oil In Porous Media", *Improved Oil Recovery by Surfactant and Polymer Flooding, Academic Press*, (1977) p. 55-91.
[13] Saffman, P.G. & Sir Geoffrey Taylor, F.R.S., "The penetration of a fluid into a porous medium or Hele-Shaw cell containing a more viscous liquid", *Dynamics of Curved Fronts, Academic Press*, (1958) **245,** p. 312-329.
[14] Melrose J.C. and Brandner C.F., "Role of Capillary Forces in Determining. Microscopic Displacement Efficiency for Oil Recovery by Waterflooding", *Enhanced Recovery*, (1974).
[15] Crouse, B., Freed, D.M., Koliha, N., Balasubramanian, G., EXA CORP, Satti, R., Bale, D., Zuklic, S., BAKER-HUGHES INC, "A Lattice-Boltzmann Based Method Applied to Digital Rock Characterization of Perforation Tunnel Damage", *SCA Symposium*, (2016).
[16] Jerauld, G.R., Fredrich, J., Lane, N., Sheng, Q., Crouse, B., Freed, D.M., … Xu, R., "Validation of a Workflow for Digitally Measuring Relative Permeability", *Society of*

Petroleum Engineers, (2017).
[17] Otomo, H., Fan, H., Hazlett, R., Li, Y., Staroselsky, I., Zhang, R., & Chen, H., "Simulation Of Residual Oil Displacement In A Sinusoidal Channel With The Lattice Boltzmann Method", *Comptes Rendus Mécanique*, (2015) **343**, 10, 559–570.
[18] Otomo, H., Fan, H., Li, Y., Dressler, M., Staroselsky, I., Zhang, R., & Chen, H., "Studies Of Accurate Multi-Component Lattice Boltzmann Models On Benchmark Cases Required For Engineering Applications", *Journal of Computational Science,* (2016) **17,** Part 2, 334–339.
[19] Shan, X., & Chen, H., "Lattice Boltzmann Model For Simulating Flows With Multiple Phases And Components", *Physical Review E*, (1993). **47**, 3, 1815.
[20] Otomo, H., Crouse, B., Dressler, M., Freed, D.M., Staroselsky, I., Zhang, R., & Chen, H., "Multi-Component Lattice Boltzmann Models For Accurate Simulation Of Flows With Wide Viscosity Variation", *Computers & Fluids*, (2018).
[21] Chen, H., Teixeira, C., & Molvig, K., "Realization Of Fluid Boundary Conditions Via Discrete Boltzmann Dynamics", *Intl. J. Mod. Phys. C* (1998) **9**, p. 1281-1292.
[22] Shan, X., Yuan, X. & Chen, H., "Kinetic Theory Representation Of Hydrodynamics: A Way Beyond The Navier-Stokes Equation", *J. Fluid Mech.*, (2006) **550**, p. 413-441.
[23] Zhang, R., Shan, X. & Chen, H., "Efficient Kinetic Method For Fluid Simulation Beyond The Navier-Stokes Equation", *Physical Review E*, (2006) **74**, 046703
[24] Chen, H., Zhang, R. & Gopolakrishnan, P. "Lattice Boltzmann Collision Operators Enforcing Isotropy And Galilean Invariance", US Patent US9576087B2, (2013).
[25] Andra, H., Combaret, N., Dvorkin, J. … Zhan, X, "Digital rock physics benchmarks—Part I: Imaging and segmentation", *Computers & Geosciences*. (2012) **50**, p. 25–32
[26] Amott, E., "Observations Relating to the Wettability of Porous Rock", *Society of Petroleum Engineers*. (1959)
[27] Jadhunandan, P. P., and N. R. Morrow, "Effect of wettability on waterflood recovery for crude-oil/brine/rock systems", *SPE Reservoir Eng.*, (1995) **10**(1), p. 40–46.